Journal of the Mechanics and Physics of Solids 59 (2011) 1808–1822

Contents lists available at ScienceDirect

Journal of the Mechanics and Physics of Solids

journal homepage: www.elsevier.com/locate/jmps

Prediction of the softening and damage effects with permanent set in fibrous biological materials

Estefanía Peña [a,b,*]

[a] Aragón Institute of Engineering Research (I3A), University of Zaragoza, María de Luna, 3. E-50018 Zaragoza, Spain
[b] CIBER de Bioingeniería, Biomateriales y Nanomedicina (CIBER-BBN), Spain

ARTICLE INFO

Article history:
Received 13 January 2011
Received in revised form
22 May 2011
Accepted 28 May 2011
Available online 2 June 2011

Keywords:
Hyperelasticity
Constitutive modeling
Damage mechanics
Mullins type behavior
Soft tissues

ABSTRACT

Deformation induced softening is an inelastic phenomenon frequently accompanying mechanical response of soft biological tissues. Inelastic phenomena which occur in mechanical testing of biological tissues are very likely to be associated with alterations in the internal structure of these materials.

In this study, a novel structural constitutive model is formulated to describe the inelastic effects in soft biological tissues such as Mullins type behavior, damage and permanent set as a result of residual strains after unloading. Anisotropic softening is considered by evolution of internal variables governing the anisotropic properties of the material. We consider two weight factors w_i (softening) and s_k (discontinuous damage) as internal variables characterizing the structural state of the material. Numerical simulations of several soft tissues are used to demonstrate the performance of the model in reproducing the inelastic behavior of soft biological tissues.

1. Introduction

Enormous progress has been made during recent years in the phenomenological modeling of soft tissue (Fung, 1993; Zhou and Fung, 1997; Holzapfel et al., 2000; Humphrey, 2002). In general, three important softening phenomena associated with biological tissues may be distinguished. First, there is the dependence of the mechanical response on the previously attained maximum load level. This is very similar to the well-known Mullins effect in rubber-like materials (Franceschini et al., 2006; Alastrué et al., 2008; Peña et al., 2011a). Another typical phenomenon known as permanent set is characterized by residual strains after unloading (Alastrué et al., 2008; Muñoz et al., 2008; Peña et al., 2011a). Finally, there is a failure behavior resulting from fiber rupture and matrix disruption associated with material damage and fracture due to the micro-cracks that are produced in the tissue during the load process (Volokh, 2007b; Calvo et al., 2009; Peña et al., 2010).

There are several constitutive models able to describe the failure of soft tissues (Hokanson and Yazdami, 1997; Hurschler et al., 1997; Natali et al., 2005; Wulandana and Robertson, 2005; Balzani et al., 2006; Rodríguez et al., 2006; Volokh, 2007a; Vita and Slaughter, 2007; Volokh and Vorp, 2008; Li and Robertson, 2009; Ciarletta and Ben-Amar, 2009). Balzani et al. (2006) assumed that discontinuous damage occurs in arterial walls and mainly along the fiber direction. Rodríguez et al. (2006, 2008a) introduced a stochastic-structurally based damage model for fibrous soft tissues. Only a few constitutive models have been derived to describe the loading–unloading softening behavior of soft tissues (Franceschini

* Correspondence address: Aragón Institute of Engineering Research (I3A), University of Zaragoza, María de Luna, 3. E-50018 Zaragoza, Spain. Tel.: +34 976761912; fax: +34 976762578.
E-mail address: fany@unizar.es

0022-5096/$ - see front matter © 2011 Elsevier Ltd. All rights reserved.
doi:10.1016/j.jmps.2011.05.013

et al., 2006; Calvo et al., 2007; Rodríguez et al., 2008a; Ehret and Itskov, 2009; Peña and Doblare, 2009; Li and Robertson, 2009; Peña et al., 2009). Franceschini et al. (2006) and Horgan and Saccomandi (2005) proposed an isotropic pseudo-elastic model for soft tissues using isotropic and anisotropic elastic strain-energy functions respectively. Calvo et al. (2007) proposed an uncoupled directional damage model for fibered biological soft tissues that considers different damage evolutions for the matrix and for the different fiber families. In Li and Robertson (2009) two damage mechanisms are coupled in a multiplicative manner. Peña et al. (2009) showed that continuum damage mechanics models can reproduce the softening behavior during unloading or reloading only for low dissipative effects. Ehret and Itskov (2009) presented a model that reproduces the softening behavior including all the tissue dissipative effects (permanent set also). However, the main drawback of this model is its use of non-standard invariants that leads to a very complicated approach. The model is not able to reproduce the damage process. Peña and Doblare (2009) present a very simple pseudo-elastic anisotropic model to reproduce the softening behavior exhibited in soft biological tissues without permanent set. However the pseudo-elastic model is not able to reproduce the failure region as a result of the bond rupture and complete damage while continuum damage mechanics (CDM) and other models can.

In this study, a novel structural constitutive model is formulated to describe the softening effects in soft biological tissues such as Mullins type behavior, damage and permanent set as a result of residual strains after unloading. We consider two weight factors w_i and s_k as internal variables characterizing the structural state of the material. The model combines simplicity and applicability with relatively low number of material parameters, so it is a good candidate for modeling stress-softening in biological soft tissues.

The paper is organized as follows. In Section 2 the constitutive equations of finite elasticity with uncoupled volume response are briefly reviewed. We represent the free-energy density function for biological tissues in a generalized form. In Section 3 the phenomenological inelastic model including evolution equations for the internal variables is presented. The application of this model to some examples is presented in Section 4. Comparisons with experimental data and numerical simulations are included to illustrate the effectiveness of the proposed formulation. Finally, Section 5 includes some concluding remarks, followed by an appendix that summarizes the derivation of the stress and the elastic tangent tensor.

2. Basic results in continuum mechanics for hyperelastic media

2.1. Finite elasticity with uncoupled volume response

Let $\mathcal{B}_0 \subset \mathbb{R}^3$ be a reference or rather material configuration of a body B of interest. The notation $\boldsymbol{\chi} : \mathcal{B}_0 \times \mathcal{T} \to \mathcal{B}_t$ represents the one to one mapping, continuously differentiable, transforming a material point $\mathbf{X} \in \mathcal{B}_0$ to a position $\mathbf{x} = \boldsymbol{\varphi}(\mathbf{X},t) \in \mathcal{B}_t \subset \mathbb{R}^3$, where $\mathcal{B}_t$ represents the deformed configuration at time $t \in \mathcal{T} \subset \mathbb{R}$. The mapping $\boldsymbol{\chi}$ represents a motion of the body B that establishes the trajectory of a given point when moving from its reference position $\mathbf{X}$ to $\mathbf{x}$. The two-point deformation gradient tensor is defined as $\mathbf{F} = \nabla\boldsymbol{\chi}(\mathbf{X},t) : \mathrm{T}\mathcal{B}_0 \to \mathrm{T}\mathcal{B}_t$ that defines the linear tangent map from the material tangent space $\mathrm{T}\mathcal{B}_0$ to the spatial tangent space $\mathrm{T}\mathcal{B}_t$, with $J(\mathbf{X}) = \det(\mathbf{F}) > 0$ the local volume variation and $\mathbf{C} = \mathbf{F}^T\mathbf{F}$ the corresponding right Cauchy–Green tensor as a characteristic material deformation measure.

It is sometimes useful to consider the multiplicative decomposition of $\mathbf{F} = J^{1/3}\mathbf{I} \cdot \overline{\mathbf{F}}$. Hence, deformation is split into a dilatational part, $J^{1/3}\mathbf{I}$, where $\mathbf{I}$ represents the second-order identity tensor, and an isochoric contribution, $\overline{\mathbf{F}}$, so that $\det(\overline{\mathbf{F}}) = 1$ (Flory, 1961; Simo and Taylor, 1991). With these quantities at hand, the isochoric counterparts of the right Cauchy–Green deformation tensor associated with $\overline{\mathbf{F}}$ is defined as $\overline{\mathbf{F}} := \overline{\mathbf{F}}^{\mathrm{T}} \cdot \overline{\mathbf{F}} = J^{-2/3}\mathbf{C}$. For materials with two directions of anisotropy, a typical representation of biological soft tissues, it is necessary to introduce two unit vectors $\mathbf{m}_0$ and $\mathbf{n}_0$ describing the anisotropy direction, and the concept of pseudo-invariants, describing the invariants associated to this vector and the deformation tensor, Fig. 1. Therefore, the following invariants and pseudo-invariants were used (Peña et al., 2009)

$$\bar{I}_4 = \overline{\mathbf{C}} : \mathbf{M} = \bar{\lambda}_m^2, \quad \bar{I}_5 = \overline{\mathbf{C}}^2 : \mathbf{M}, \quad \bar{I}_6 = \overline{\mathbf{C}} : \mathbf{N} = \bar{\lambda}_n^2 \tag{1}$$

$$\bar{I}_7 = \overline{\mathbf{C}}^2 : \mathbf{N}, \quad \bar{I}_8 = [\mathbf{m}_0 \cdot \mathbf{n}_0]\mathbf{m}_0 \cdot \overline{\mathbf{C}}\mathbf{n}_0, \quad \bar{I}_9 = [\mathbf{m}_0 \cdot \mathbf{n}_0]^2$$

where $\mathbf{M} = \mathbf{m}_0 \otimes \mathbf{m}_0$ and $\mathbf{N} = \mathbf{n}_0 \otimes \mathbf{n}_0$ are structural tensors. It is important to remark the problematic nature of the Flory decomposition in the cases of the fiber-reinforced materials is some cases, see Helfenstein et al. (2010).

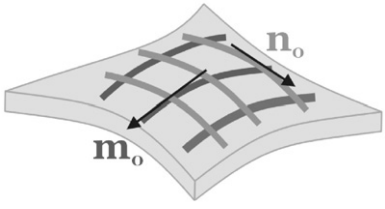

Fig. 1. Schematic representation of a simplified biological tissue.

To characterize isothermal processes, we postulate the existence of a unique decoupled representation of the strain-energy density function Ψ (Simo et al., 1985). Because of the directional dependence on the deformation, we require that the function Ψ explicitly depends on both the right Cauchy–Green tensor $\mathbf{C}$ and the fiber directions $\mathbf{m}_0$ and $\mathbf{n}_0$ in the reference configuration. Since the sign of $\mathbf{m}_0$ and $\mathbf{n}_0$ is not significant, Ψ must be an even function of $\mathbf{m}_0$ and $\mathbf{n}_0$ and so it may be expressed by $\Psi=\Psi(\mathbf{C},\mathbf{M},\mathbf{N})$ (Spencer, 1971). Based on the kinematic description, the free energy can be rewritten in decoupled form as

$$\Psi(\mathbf{C},\mathbf{M},\mathbf{N})=\Psi_{\text{vol}}(J)+\Psi_{\text{ich}}(\overline{\mathbf{C}},\mathbf{M},\mathbf{N}) \tag{2}$$

where $\Psi_{\text{vol}}(J)$ and $\Psi_{\text{ich}}(\overline{\mathbf{C}},\mathbf{M},\mathbf{N})$ are given scalar-valued functions of J, $\overline{\mathbf{C}}$, $\mathbf{m}_0$ and $\mathbf{n}_0$ respectively that describe the volumetric and isochoric responses of the material (Holzapfel, 2000). This strain-energy density function must satisfy the principle material frame invariance $\Psi(\mathbf{C},\mathbf{M},\mathbf{N})=\Psi(\mathbf{Q}\cdot\mathbf{C},\mathbf{Q}\cdot\mathbf{M},\mathbf{Q}\cdot\mathbf{N})$ for all $[\mathbf{C},\mathbf{Q}]\in[\mathbb{S}^3_+\times\mathbb{Q}^3_+]$.

In terms of the strain invariants Ψ can be written as

$$\Psi=\Psi_{\text{vol}}(J)+\Psi_{\text{ich}}(\overline{I}_1,\overline{I}_2,\overline{I}_4,\overline{I}_5,\overline{I}_6,\overline{I}_7,\overline{I}_8) \tag{3}$$

Remark 2.1. While the invariants $\overline{I}_4$ and $\overline{I}_6$ have a clear physical meaning, the square of the stretch λ in the fiber directions, the influence of $\overline{I}_5$, $\overline{I}_7$ and $\overline{I}_8$ is difficult to evaluate due to the high correlation between them (Holzapfel and Ogden, 2009). For this reason and because of the lack of sufficient experimental data it is usual not to include these invariants in the definition of Ψ. Finally, $\overline{I}_9$ does not depend on the deformation, so it has not been included in (3).

The second Piola–Kirchhoff stress tensor is obtained by derivation of (2) with respect to the right Cauchy–Green tensor. Thus, the stress tensor consists of a purely volumetric and a purely isochoric contribution, i.e. $\mathbf{S}_{\text{vol}}$ and $\mathbf{S}_{\text{ich}}$, so the total stress is

$$\begin{aligned}\mathbf{S}&=\mathbf{S}_{\text{vol}}+\mathbf{S}_{\text{ich}}=2\frac{\partial\Psi_{\text{vol}}(J)}{\partial\mathbf{C}}+2\frac{\partial\Psi_{\text{ich}}(\overline{\mathbf{C}},\mathbf{M},\mathbf{N})}{\partial\mathbf{C}}=2\left[\frac{\partial\Psi_{\text{vol}}(J)}{\partial J}\frac{\partial J}{\partial\mathbf{C}}+\frac{\partial\Psi_{\text{ich}}(\overline{\mathbf{C}},\mathbf{M},\mathbf{N})}{\partial\overline{\mathbf{C}}}\frac{\partial\overline{\mathbf{C}}}{\partial\mathbf{C}}\right]\\&=Jp\mathbf{C}^{-1}+2\sum_{j=1,2,4,6}\mathbf{P}:\frac{\partial\Psi_{\text{ich}}}{\partial\overline{I}_j}\frac{\partial\overline{I}_j}{\partial\overline{\mathbf{C}}}\end{aligned} \tag{4}$$

Moreover, one obtains the following noticeable relations $\partial_{\mathbf{C}}J=\frac{1}{2}J\mathbf{C}^{-1}$ and $\mathbf{P}=\partial_{\mathbf{C}}\overline{\mathbf{C}}=J^{-2/3}[\mathbf{I}-\frac{1}{3}\mathbf{C}\otimes\mathbf{C}^{-1}]$. $\mathbf{P}$ is the fourth-order projection tensor and $\mathbf{I}$ denotes the fourth-order unit tensor, which, in index notation, has the form $\mathrm{I}_{IJKL}=\frac{1}{2}[\delta_{IK}\delta_{JL}+\delta_{IL}\delta_{JK}]$. Application of the fourth-order projection tensor $\mathbf{P}$ furnishes the physically correct deviatoric operator in the Lagrangian description, so that $[\mathbf{P}:(\cdot)]:\mathbf{C}=\mathbf{0}$ (Federico, 2010). Note that it is possible to obtain the Cauchy stress tensor by applying the push-forward operation to (4) $\boldsymbol{\sigma}=J^{-1}\boldsymbol{\chi}_*(\mathbf{S})$ (Marsden and Hughes, 1994).

Based on the kinematic decomposition of the deformation gradient tensor, the tangent operator, also known as the elasticity tensor when dealing with elastic constitutive laws, is defined in the reference configuration as

$$\mathbf{C}=2\frac{\partial\mathbf{S}(\mathbf{C},\mathbf{M},\mathbf{N})}{\partial\mathbf{C}}=\mathbf{C}_{\text{vol}}+\mathbf{C}_{\text{ich}}=4\left[\frac{\partial^2\Psi_{\text{vol}}(J)}{\partial\mathbf{C}\otimes\partial\mathbf{C}}+\frac{\partial^2\Psi_{\text{ich}}(\overline{\mathbf{C}},\mathbf{M},\mathbf{N})}{\partial\mathbf{C}\otimes\partial\mathbf{C}}\right] \tag{5}$$

Note that its spatial counterpart of (5) is obtained from the application of the push-forward operation to (5) $\mathbf{c}=J^{-1}\boldsymbol{\chi}_*(\mathbf{C})$ (Holzapfel, 2000). Close-form expression for $\mathbf{C}$ for the particular SEF proposed in this work are given in Appendix B.

2.2. Generalized form for the strain-energy function

The mechanical tests on soft biological tissues show a J-shaped stress mechanical response that is well described by an exponential representation. For this reason, we consider a general deviatoric strain-energy function (SEF) decoupled in matrix $\Psi^{\text{mat}}_{\text{ich}}$ and fiber $\Psi^{\text{fib}}_{\text{ich}}$ contributions:

$$\begin{aligned}\Psi_{\text{ich}}(\overline{\mathbf{C}},\mathbf{M},\mathbf{N})&=\Psi^{\text{mat}}_{\text{ich}}(\overline{\mathbf{C}})+\Psi^{\text{fib}}_{\text{ich}}(\overline{\mathbf{C}},\mathbf{M},\mathbf{N})\\&=\mu_1[\overline{I}_1-3]+\mu_2[\overline{I}_2-3]+\frac{\gamma}{a\eta}[\exp(\eta[\overline{I}_1-3]^a)-f(\overline{I}_1,a)]+\sum_{i=4,6}\frac{c_{i-3}}{bc_{i-2}}[\exp(c_{i-2}[\overline{I}_i-\overline{I}_{i_0}]^b)-g(\overline{I}_i,\overline{I}_{i_0},b)]\end{aligned} \tag{6}$$

where μ_1 and μ_2 are stress-like parameters of the matrix (corresponding to a Mooney–Rivlin SEF with the condition $\mu_1+\mu_2\geq 0$ (Ogden, 1996)), γ and $c_{i-3}>0$ are stress-like and η and $c_{i-2}>0$ dimensionless parameters associated to the matrix and fibers, respectively. $\overline{I}_i$ ($i=4,6$) characterize the mechanical response in the anisotropy directions (Holzapfel et al., 2000) and $\overline{I}_{i_0}>1$ are dimensionless parameters regarded as the initial crimping of the fibers (Rodríguez et al., 2008b). Moreover, it has been assumed that the SEF corresponding to the anisotropic terms ($\Psi^{\text{fib}}_{\text{ich}}$) only contributes to the global mechanical response of the tissue when stretched, that is, $\overline{I}_i>\overline{I}_{i_0}$. a and b are parameters related with the degree of the exponential function ($a,b=0,1,2$) and $f(\overline{I}_1,a)$ and $g(\overline{I}_i,\overline{I}_{i_0},b)$ are energy-like functions to enforce the essential conditions of a SEF ($\Psi_{\text{ich}}(\mathbf{1},\mathbf{M},\mathbf{N})=0,\mathbf{S}_{\text{ich}}(\mathbf{1},\mathbf{M},\mathbf{N})=\mathbf{0}$).

Remark 2.2. The particular expressions of (6) for the classical SEF for biological tissues are the following

- For isotropic materials, $\gamma, c_{i-3}=0$, the SEF is the well-known Mooney–Rivlin equation (Mooney, 1940).

$$\Psi_{\text{ich}}(\overline{\mathbf{C}})=\mu_1[\bar{I}_1-3]+\mu_2[\bar{I}_2-3] \tag{7}$$

- Another isotropic constitutive law for vascular tissues obtained from (6) using $\mu_1=0$, $\mu_2=0$, $a=1$, $c_{i-3}=0$ and $f=-1$ was developed by Demiray (1972)

$$\Psi_{\text{ich}}(\overline{\mathbf{C}})=\frac{\gamma}{\eta}[\exp(\eta[\bar{I}_1-3])-1]. \tag{8}$$

This strain-energy density function that was modified in a later contribution (Demiray et al., 1988) by including a neo-Hookean term and the quadratic dependence of the term $[\bar{I}_1-3]$ in (8) are obtained using $\mu_2=0$, $a=2$, $c_{i-3}=0$ and $f=-1$

$$\Psi_{\text{ich}}(\overline{\mathbf{C}})=\mu_1[\bar{I}_1-3]+\frac{\gamma}{2\eta}[\exp(\eta[\bar{I}_1-3]^2)-1], \tag{9}$$

- The transversely isotropic model by Natali et al. (2003) specifically designed for tendons and ligaments is obtained using $\mu_2=0$, $\gamma=0$, $b=1$, $i=4$, $\bar{I}_{4_0}=1$, and $g=c_2[\bar{I}_4-1]-1$

$$\Psi_{\text{ich}}(\overline{\mathbf{C}},\mathbf{M})=\mu_1[\bar{I}_1-3]+\frac{c_1}{c_2}[\exp(c_2[\bar{I}_4-1])-c_2[\bar{I}_4-1]-1] \tag{10}$$

- The classical model that includes two directions of anisotropy, specifically designed for the arterial tissue and developed by Holzapfel et al. (2000) is obtained using $\mu_2=0$, $\gamma=0$, $b=2$, $\bar{I}_{i_0}=1$ and $g_i=-1$

$$\Psi_{\text{ich}}(\overline{\mathbf{C}},\mathbf{M},\mathbf{N})=\mu_1[\bar{I}_1-3]+\frac{c_1}{2c_2}[\exp(c_2[\bar{I}_4-1]^2)-1]+\frac{c_3}{2c_4}[\exp(c_4[\bar{I}_6-1]^2)-1] \tag{11}$$

- For the well-known Weiss's SEF (Weiss et al., 1996) specifically designed for tendons and ligaments that was modified in order to obtain an analytical expression for the strain-energy function (Calvo et al., 2009), the previous representation is

$$\Psi_{\text{ich}}(\overline{\mathbf{C}})=\mu[\bar{I}_1-3]+\gamma[\bar{I}_2-3]+\Psi_{\text{ich(f)}}$$

$$\Psi_{\text{ich(f)}}(\overline{\mathbf{C}},\mathbf{M},\mathbf{N})=0 \quad \bar{I}_i<\bar{I}_{i_0}$$

$$\Psi_{\text{ich(f)}}(\overline{\mathbf{C}},\mathbf{M},\mathbf{N})=\sum_{i=4,6}\frac{c_{i-3}}{c_{i-2}}[\exp(c_{i-2}[\bar{I}_i-\bar{I}_{i_0}])-c_{i-2}[\bar{I}_i-\bar{I}_{i_0}]-1] \quad \bar{I}_i>\bar{I}_{i_0} \text{ and } \bar{I}_i<\bar{I}_{i_{ref}}$$

$$\Psi_{\text{ich(f)}}(\overline{\mathbf{C}},\mathbf{M},\mathbf{N})=c_{i-1}\sqrt{\bar{I}_i-\bar{I}_{i_0}}+c_i\ln(\bar{I}_i-\bar{I}_{i_0})+c_{i+1} \quad \bar{I}_i>\bar{I}_{i_{ref}} \tag{12}$$

$\bar{I}_{i_{ref}}$ characterizes the stretch at which collagen fibers start to be straightened, c_{i-1}, and c_i are stress-like parameters, and c_{i+1} are an energy-like parameter.

It has been experimentally observed that the collagen fibers in a relaxed tissue appear to be wavy and crimped (Baer et al., 1991; Diamant et al., 1972). Thus, they sustain little load in the initial stage of the stretching of the tissue. This is reflected by the toe region of the tensile stress–strain curve of the tissue which is characterized by a small tangent modulus (Tang and Moran, 2009). Furthermore, the material parameters $\bar{I}_{i_0}$ in (6) are a critical value related to the secondary stiffening of the fiber (Tang and Moran, 2009). To include this effect, in this paper we consider the two following SEFs that correspond to the particularized form of (6)

- The transversely isotropic model by Natali et al. (2003), named the *Exponential model (Exp)*, specifically designed for tendons and ligaments, is modified by

$$\Psi_{\text{ich}}(\overline{\mathbf{C}},\mathbf{M})=\mu[\bar{I}_1-3]+\frac{c_1}{c_2}[\exp(c_2[\bar{I}_4-\bar{I}_{4_0}])-c_2[\bar{I}_4-\bar{I}_{4_0}]-1] \tag{13}$$

where μ is a stress-like parameter of the matrix (corresponding to a neo-Hookean SEF with the condition $\mu\geq 0$ (Ogden, 1996)), $c_1>0$ is a stress-like and $c_2>0$ a dimensionless parameter associated to the fibers. Moreover, it has been assumed that the strain-energy corresponding to the anisotropic terms only contributes to the global mechanical response of the tissue when stretched, that is, $\bar{I}_4>\bar{I}_{4_0}$.

- On the other hand, the classical model that include two directions of anisotropy, specifically designed for the arterial tissue developed by Holzapfel et al. (2000) and later modified by Rodríguez et al. (2008b), named the

quadratic exponential model (QExp), is also obtained

$$\Psi_{\text{ich}}(\overline{\mathbf{C}},\mathbf{M},\mathbf{N}) = \mu[\bar{I}_1-3]+\frac{k_1}{2k_2}[\exp(k_2[\bar{I}_4-\bar{I}_{4_0}]^2)-1]+\frac{k_3}{2k_4}[\exp(k_4[\bar{I}_6-\bar{I}_{6_0}]^2)-1] \tag{14}$$

where $k_1>0$ and $k_3>0$ are stress-like, and $k_2>0$ and $k_4>0$ are dimensionless parameters associated to the fibers, while $\bar{I}_{4_0}>1$ and $\bar{I}_{6_0}>1$ characterize the stretch at which collagen fibers start to be stretched.

3. A phenomenological inelastic model

The experimental results suggest that just like the elastic properties, the inelastic behavior of soft tissues is also characterized by anisotropy (Alastrué et al., 2008; Peña et al., 2009, 2010, 2011a). Accordingly, a suitable constitutive model should account for this directional dependence and take into account the different alteration mechanisms associated with this anisotropy. The phenomenological inelastic model should include the Mullins effect, the permanent set resulting from the residual strains after unloading, and the fiber and matrix disruption associated to supraphysiological loads or strains (Calvo et al., 2009).

To model these inelastic processes, we apply the following considerations:

- In Section 2.2 we have introduced the $\bar{I}_{i_0}$ parameter that governs the anisotropic contribution to the global mechanical response of the tissue only when stretched, that is, $\bar{I}_i>\bar{I}_{i_0}$. We modified this parameter by a weight factor w_i associated to $\bar{I}_{i_0}$ that changes independently from each direction to take into account structural alterations along the fiber direction, that is, $w_i\cdot\bar{I}_{i_0}$. With this modification, we can reproduce at the same time the softening behavior and the permanent set presented in this kind of tissue.
- Finally, the softening as a result of the bond rupture and complete damage is accomplished by using the classical continuum damage mechanics (CDM) theory using the well-known reduction factors (Simo and Ju, 1987), D_k, associated to the matrix ($\bar{I}_1$ and $\bar{I}_2$) and the fibers ($\bar{I}_i$) (Calvo et al., 2007).

In the following, we consider the weight factors w_i and D_k as internal variables characterizing the structural state of the material. With these considerations in mind, the free energy for the material is assumed to be of the form:

$$\Psi(\mathbf{C},\mathbf{M},\mathbf{N},D_k,w_i) = \Psi_{\text{vol}}(J)+[1-D_m]\Psi^{\text{mat}}_{\text{ich}}(\overline{\mathbf{C}})+\sum_{i=f_4,f_6}[1-D_i]\Psi^{\text{fib(i)}}_{\text{ich}}(\overline{\mathbf{C}},\mathbf{M},\mathbf{N},w_i) \tag{15}$$

where $[1-D_k]$ $(k=m,f_4,f_6)$ are the reduction factors (Simo and Ju, 1987), $D_k:\mathbb{R}_+\to\mathbb{R}_+$ being normalized scalars referred to as the damage variables where D_k are monotonically increasing smooth functions with the properties $D_k(0)=0$ and $D_k(s_k)\in[0,1]\ \forall\ s_k$ where s_k are the internal variables that control the damage D_k. These can be considered as shape functions which relate the damage variables D_k with the internal variables s_k which describe the discontinuous damage (Peña et al., 2009).

Particularizing (15) to the SEF proposed in (13) and (14) we obtain for the *Exp* model

$$\Psi_{\text{ich}}(\overline{\mathbf{C}},\mathbf{M},D_m,D_{f_4},w_4) = \mu[1-D_m][\bar{I}_1-3]+[1-D_{f_4}]\frac{c_1}{c_2}[\exp(c_2[\bar{I}_4-w_4\bar{I}_{4_0}])-c_2[\bar{I}_4-w_4\bar{I}_{4_0}]-1] \tag{16}$$

and for *QExp* model

$$\Psi_{\text{ich}}(\overline{\mathbf{C}},\mathbf{M},\mathbf{N},D_k,w_i) = \mu[1-D_m][\bar{I}_1-3]+[1-D_{f_4}]\frac{k_1}{2k_2}[\exp(k_2[\bar{I}_4-w_4\bar{I}_{4_0}]^2)-1]+[1-D_{f_6}]\frac{k_3}{2k_4}[\exp(k_4[\bar{I}_6-w_6\bar{I}_{6_0}]^2)-1] \tag{17}$$

The second law of thermodynamics asserts a non-negative rate of entropy production. Using standard arguments based on the Clausius–Duhem inequality (Marsden and Hughes, 1994):

$$\mathcal{D}_{int} = -\dot{\Psi}+\frac{1}{2}\mathbf{S}:\dot{\mathbf{C}}\geq 0 \tag{18}$$

yields

$$\mathcal{D}_{int} = \left[\mathbf{S}-J\frac{d\Psi^0_{\text{vol}}(J)}{dJ}\mathbf{C}^{-1}-2J^{\frac{-2}{3}}\sum_{k=m,f_4,f_6}\mathbf{P}:[1-D_k]\frac{\partial\Psi^0_{\text{ich(k)}}}{\partial\mathbf{C}}\right]:\frac{\dot{\overline{\mathbf{C}}}}{2}-\left[\sum_{k=m,f_4,f_6}\frac{\partial\Psi_{\text{ich(k)}}}{\partial D_k}\dot{D}_k+\sum_{i=f_4,f_6}\frac{\partial\Psi_{\text{ich(i)}}}{\partial w_i}\dot{w}_i\right]\geq 0 \tag{19}$$

where the thermodynamic forces are

$$f_{d_k} = -\frac{\partial\Psi_{\text{ich(k)}}}{\partial D_k} = \Psi^0_{\text{ich(k)}}\geq 0,\quad f_{w_i} = -\frac{\partial\Psi_{\text{ich(i)}}}{\partial w_i} = \bar{f}_i\frac{\partial\Psi_{\text{ich(i)}}}{\partial\bar{I}_i}\geq 0 \tag{20}$$

with $\Psi^0_{\text{ich(k)}}(k=m,f_4,f_6)$ being the contributions of the matrix and the two families of fibers respectively in undamaged cases (with softening) named effective strain-energy and $(i=f_4,f_6)$.

Remark 3.1. To compute f_{w_i}, it is necessary to obtain the expression of $\bar{f}_i$ for each strain-energy function (SEF).

For the *Exp* model we obtain where $i=f_4$

$$f_{w_{f_4}} = -\frac{\partial \Psi_{\text{ich(f4)}}}{\partial w_4} = [1-D_{f_4}]c_1\bar{I}_{40}[\exp(c_2[\bar{I}_4 - w_4\bar{I}_{4_0}])-1] = \bar{I}_{40}\frac{\partial \Psi_{\text{ich(f4)}}}{\partial \bar{I}_4} \geq 0 \tag{21}$$

And for the *QExp* SEF the thermodynamic force is derived as

$$f_{w_i} = -\frac{\partial \Psi_{\text{ich(i)}}}{\partial w_i} = [1-D_i]k_1\bar{I}_{i0}[\bar{I}_i - w_i\bar{I}_{i0}][\exp(c_2[\bar{I}_i - w_i\bar{I}_{i_0}]^2)-1] = \bar{I}_{i0}\frac{\partial \Psi_{\text{ich(i)}}}{\partial \bar{I}_i} \geq 0 \tag{22}$$

So, in this particular case, using a compact formulation, for each strain-energy function $\bar{f}_i = \bar{I}_{i0}$.

The first term in (18) determines the second Piola–Kirchhoff stress as

$$\begin{aligned}\mathbf{S}(\mathbf{C},\mathbf{M},\mathbf{N},D_k,w_i) &= 2\frac{\partial \Psi(\mathbf{C},\mathbf{M},\mathbf{N},D_k,w_i)}{\partial \mathbf{C}} = \mathbf{S}_{\text{vol}} + \sum_{k=m f_4 f_6}[1-D_k]\mathbf{S}_{\text{ich}} = \mathbf{S}_{\text{vol}} + [1-D_m]\mathbf{S}_{\text{ich}}^{\text{mat}} + \sum_{i=f_4 f_6}[1-D_i]\mathbf{S}_{\text{ich}}^{\text{fib}} \\ &= \mathbf{S}_{\text{vol}} + [1-D_m]2\frac{\partial \Psi_{\text{ich}}^{\text{mat}}}{\partial \mathbf{C}} + \sum_{i=f_4 f_6}[1-D_i]2\frac{\partial \Psi_{\text{ich}}^{\text{fib(i)}}}{\partial \mathbf{C}}\end{aligned} \tag{23}$$

where $\mathbf{S}_{\text{vol}}$ and $\mathbf{S}_{\text{ich}}$ denote a purely volumetric and a purely isochoric effective contribution of the stress tensor of the undamaged material (4).

Remark 3.2. The softening model presented herein is particularized for quasi-incompressible materials. For incompressible materials, where $J=1$ and $\bar{\mathbf{F}}=\mathbf{F}$, the anisotropic softening model is described by

$$\Psi(\mathbf{C},\mathbf{M},\mathbf{N},D_k,w_i) = [1-D_m]\Psi^{\text{mat}}(\mathbf{C}) + \sum_{i=f_4 f_6}[1-D_i]\Psi^{\text{fib(i)}}(\mathbf{C},\mathbf{M},\mathbf{N},w_i) \tag{24}$$

and

$$\mathbf{S} = p\mathbf{C}^{-1} + [1-D_m]2\frac{\partial \Psi^{\text{mat}}}{\partial \mathbf{C}}(\mathbf{C}) + \sum_{i=f_4 f_6}[1-D_i]2\frac{\partial \Psi^{\text{fib(i)}}}{\partial \mathbf{C}}(\mathbf{C},\mathbf{M},\mathbf{N},w_i) \tag{25}$$

for derivation of the expression (25) see Bonet and Wood (2008).

Remark 3.3. Note that the discontinuous damage model can reproduce the Mullins effect in soft biological tissues (Peña et al., 2010), however, this model provides a prediction of the material response almost hyperelastic showing little inelastic dissipation (Gracia et al., 2009) due to the continuum damage mechanics model is not satisfactory for reproducing higher reduction of the stiffness. This phenomenon was already pointed out by Chagnon et al. (2004), Guo and Sluys (2006) and Gracia et al. (2009) for rubber-like materials. For this reason, in this paper the softening (Mullins effect) was associated to w_i variable and the rupture to s_k one.

3.1. Evolution of the internal variables

In the following, we are going to define the conditions for the onset and appropriate anisotropic criteria and the evolution equations for the internal variables. Motivated by approaches based on continuum damage theory (Simo, 1987; Miehe, 1995), these equations are formulated in terms of the conjugate variables f_{d_k} and f_{w_i}.

3.1.1. Discontinuous damage mechanism (D_k)

We assume that the discontinuous damage mechanism (D_k) is associated to the distortional energy and is independent of the hydrostatic pressure. Therefore, we define a damage criterion in the strain space by the condition that, at any time t of the loading process, the following expression is fulfilled (Simo, 1987)

$$\Phi_k(\bar{\mathbf{C}}(t),s_{k_t}) = \sqrt{2\Psi_{\text{ich(k)}}(\bar{\mathbf{C}}(t))} - s_{k_t} = \Xi_k - s_{k_t} \leq 0 \tag{26}$$

where $\Xi_k = \sqrt{2\Psi_{\text{ich(k)}}}$ is the equivalent energy measure (the damage energy release rate (Ju, 1989)) at time $t \in \mathbb{R}_+$ and s_{k_t} signifies the damage threshold (energy barrier) at the current time t (i.e. the radius of the damage surface) (Ju, 1989) for matrix and fibers. The equation $\Phi_k(\bar{\mathbf{C}}(t),s_{k_t})=0$ defines a damage surface in the strain space (Calvo et al., 2007).

Finally, the evolution of the damage parameters D_k is characterized by an irreversible equation of evolution

$$\dot{D}_k = \begin{cases} \bar{h}_k(\Xi_k,D_k)\dot{\mu}_k & \text{if } \Phi=0 \text{ and } \mathbf{N}_k : \dot{\bar{\mathbf{C}}} > 0 \\ 0 & \text{otherwise} \end{cases} \tag{27}$$

Here $\bar{h}_k(\Xi_k,D_{s_k})$ are given functions that characterize damage evolution in the material and $\mathbf{N}_k = \partial_{\bar{\mathbf{C}}}\Phi_k$ the normal to the damage surface in the strain space. In addition, $\dot{\mu}_k \geq 0$ is a damage consistency parameter which defines damage

loading/unloading conditions according to the Kuhn–Tucker relations:

$$\dot{\mu}_k \geq 0, \quad \Phi_k(\overline{\mathbf{C}}(t), s_{k_t}) \leq 0, \quad \dot{\mu}_k \Phi_k(\overline{\mathbf{C}}(t), s_{k_t}) = 0 \tag{28}$$

In Eqs. (28), if $\Phi_k(\Xi_k(t), s_{k_t}) \geq 0$ the damage criterion is not satisfied and by (28).c we have $\dot{\mu}_k = 0$ and no further damage takes place. On the other hand, if $\dot{\mu}_k > 0$, that is further damage is taking place, condition (28).c now implies that $\Phi_k(\Xi_k(t), s_{k_t}) = 0$. In this case, the value of $\dot{\mu}_k$ is determined by the "damage consistency condition":

$$\Phi_k(\Xi_k(t), s_{k_t}) = \dot{\Phi}_k(\Xi_k(t), s_{k_t}) = 0 \Rightarrow \dot{\mu}_k = \dot{\Xi}_k \tag{29}$$

So that s_{k_t} is given by the expression

$$s_{k_t} = \Xi_{k_t} = \max_{sr \in (-\infty, t)} \sqrt{2\Psi_{\text{ich(k)}}(\overline{\mathbf{C}}(r))} \tag{30}$$

Following previous work (Peña, in press), we consider the discontinuous damage evolution equation:

$$D_k(\Xi_{k_t}) \doteq \frac{1}{1 + \exp(-\alpha_k[\Xi_{k_t} - \gamma_k])} \tag{31}$$

with α_k and γ_k damage parameters. The parameter α_k is used to define the slope that defines the damage growth rate. That is, when α_k increases the damage evolves very fast and when the parameter α_k is very low the damage occurs more steadily, γ_k measures the center of the function, that is, when γ_k increases the energy needed to start the damage process increase.

3.1.2. Softening variables (w_i)

For the softening variables w_i, we consider the following criteria:

$$\Upsilon_i(\overline{\mathbf{C}}(t), \Gamma_{i_t}) = \frac{\partial \Psi_{\text{ich(i)}}}{\partial \overline{I}_i}(\overline{\mathbf{C}}(t), \mathbf{M}, \mathbf{N}) - \Gamma_{i_t} = \Gamma_i - \Gamma_{i_t} \leq 0 \tag{32}$$

where $\Gamma_i = \partial \Psi_{\text{ich(i)}} / \partial \overline{I}_i$ is the softening stress release rate at time $t \in \mathbb{R}_+$ and Γ_{i_t} signifies the softening threshold (stress barrier) at current time t for matrix and fibers

$$\Gamma_{i_t} = \max_{sr \in (-\infty, t)} \frac{\partial \Psi_{\text{ich(i)}}}{\partial \overline{I}_i}(\overline{\mathbf{C}}(r), \mathbf{M}, \mathbf{N}) \tag{33}$$

The equation $\Upsilon_i(\mathbf{C}(t), \Gamma_{i_t}) = 0$ defines a softening surface in the strain space. With these means at hand, we finally propose the following set of rate equations for an evolution of the softening variables:

$$\dot{w}_i \doteq \begin{cases} \dfrac{\kappa_i}{I_{i0}} \dot{\Gamma}_{i_t} & \text{if } \Upsilon = 0 \text{ and } \mathbf{N}_i : \dot{\overline{\mathbf{C}}} > 0 \\ 0 & \text{otherwise} \end{cases} \tag{34}$$

Let us now consider softening functions of the simple form:

$$w_i = \frac{\kappa_i}{I_{i0}} \Gamma_{i_t} + 1 \tag{35}$$

where κ_i is the only parameter to define the softening mechanism in each fiber direction.

Remark 3.4. Note that the softening variables $w_i \geq 1$ are not the classical normalized reduction factors $d \in [0,1]$. In the particular evolution equation of (34) $w_i \in [1, \infty)$. However it would be possible to define $\overline{w_i}$ that represents the value of w_i in the entirely softened state. For that case, the evolution equation would be

$$\dot{w}_i \doteq \begin{cases} \dfrac{\kappa_i}{I_{i0}} (\overline{w}_i - w_i) \dot{\Gamma}_{i_t} & \text{if } \Upsilon = 0 \text{ and } \mathbf{N}_i : \dot{\overline{\mathbf{C}}} > 0 \\ 0 & \text{otherwise} \end{cases} \tag{36}$$

4. Illustrative examples

In order to illustrate the performance and the physical mechanisms involved in the constitutive model presented herein, we analyzed several examples that correspond to different tissues under some typical experimental tests.

4.1. Softening parameter study

To gain a deeper insight into the effect of the different model parameters on the predicted material response, a sensitivity analysis has been carried out. Since the discontinuous damage model was previously presented in Calvo et al. (2007) and Peña et al. (2009), we only consider here the sensitivity analysis for softening mechanism. The study comprises the effect of the softening parameter κ_i defined in (35) that controls, the evolution of the softening variable w_i.

With this purpose, a uniaxial test of an incompressible biological tissue is computed in this example. Only one family of fibers is defined along the X-direction. The particular form of the SEF Ψ is defined in (16). The damage and softening evolutions are formulated in (31) and (35) respectively. To exemplify the softening model, we consider the above described sample tissue with material constants defined in Table 1. The tissue was subjected to stepwise uniaxial loading in fiber direction with five stretch controlled cycles where the stretch was 1.4, 1.6, 1.8, 2.0, 2.2.

The softening parameter κ take the values 0.01, 0.003, 0.001 and 0.0003 while the other material and damage parameters are fixed. The results show the typical characteristics of the Mullins effect and include residual stretches, see Fig. 2. We can see the influence of the parameter κ on the response of the material. First, the parameter κ has a strong influence on the permanent stretch after unloading. The results show that the permanent stretch increases as κ increases. In Fig. 2(a), where the softening parameter take the value $\kappa = 0.01$ after the third cycle the permanent set was 1.61, and for the same cycle in the materials with $\kappa = 0.003,\ 0.001,\ 0.0003$ the permanent sets obtained were 1.4, 1.1 and 1.0 (the latter means no permanent set), respectively (Fig. 2(b–d)). On the other hand, κ has a relevant influence on the maximum stress level. When κ increases the maximum stress level of the material decreases, showing the relation between softening and damage. Finally, when κ increases the stretch at total damage decreases in a similar relation with the maximum stress level. Very low values of the softening parameter κ meas that the Mullins' effect is modeled using only the discontinuous variable D_k where the softening is lower and there is no permanent set, see Fig. 2(d).

The results of the evolution of the softening internal variable w_i are presented in Fig. 3 as w_i versus stretch in the X-direction. Similarly the permanent set response, when κ increases the evolution of w_i is faster and the values of the internal variable are higher. This evolution is related to those of the softening and residual stretch mentioned above. In fact, for the lower value of the softening parameter $\kappa = 0.0003$, w_i takes a value close to 1.0 which means that there is

Table 1
Material, damage and softening parameters for uniaxial simple tension. μ and c_1 are in MPa, γ_i is in $\mathrm{MPa}^{1/2}$ and other parameter are dimensionless.

μ	c_1	c_2	I_{4_0}	
0.018	2.1226	1.5973	1.0	
α_m	γ_m	α_f	γ_f	κ
6.5	0.6	0.9	6.75	0.01/0.003/0.001/0.0003

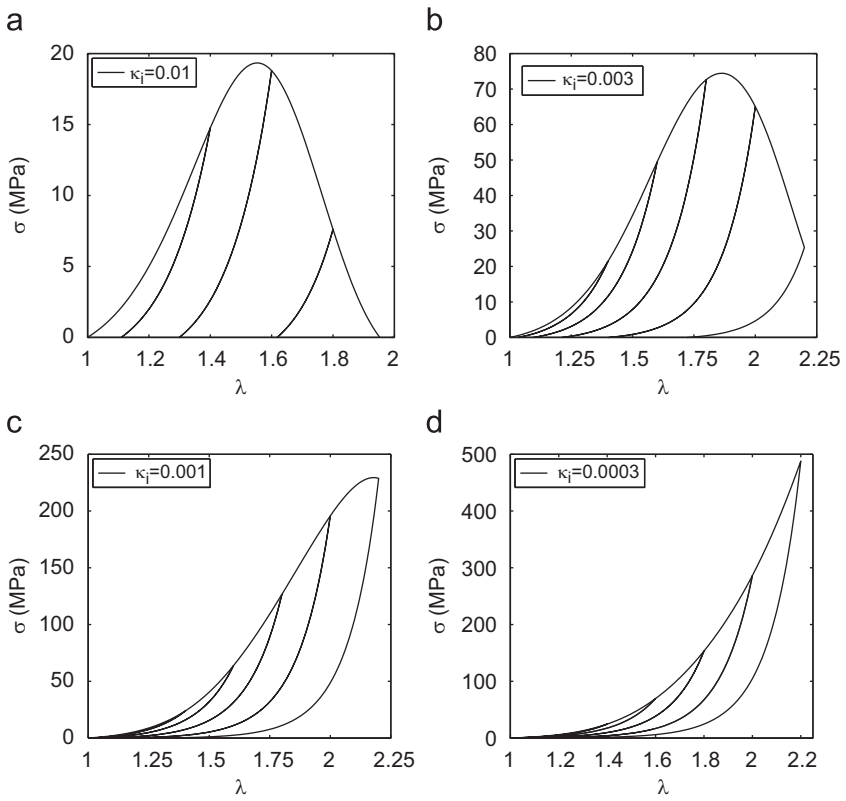

Fig. 2. Uniaxial stress response under cyclic uniaxial tension for different values of $\kappa = [0.01, 0.003, 0.001, 0.0003]$.

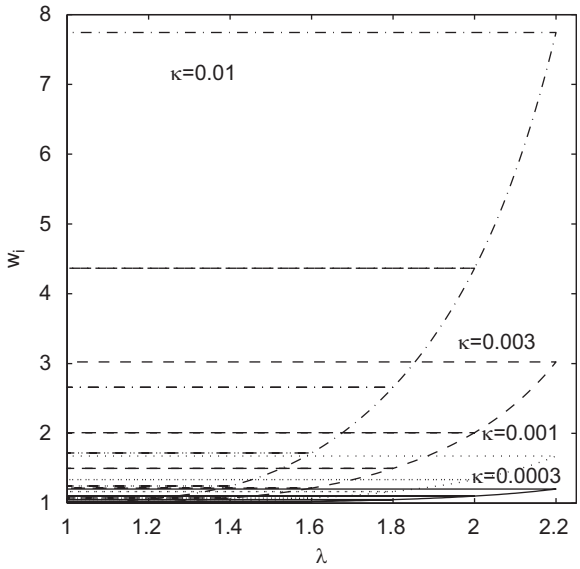

Fig. 3. Softening variable evolution for different values of $\kappa = [0.01, 0.003, 0.001, 0.0003]$.

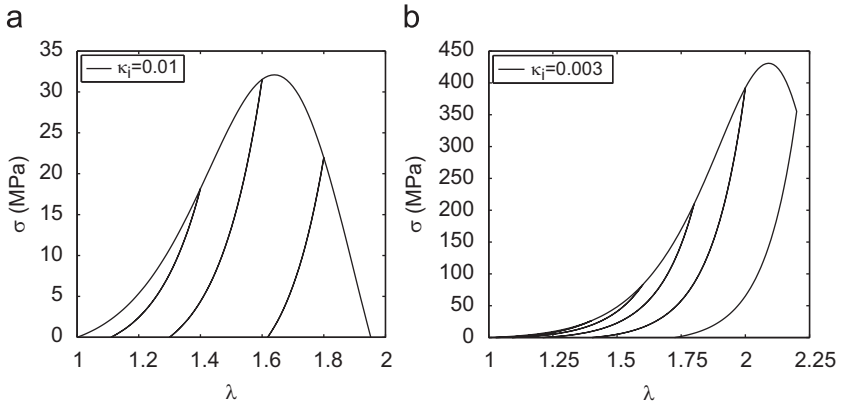

Fig. 4. Uniaxial stress response under cyclic uniaxial tension for different values of $\kappa = [0.01, 0.003]$ without discontinuous damage.

very little softening and residual stretch. Finally, in Fig. 3 it is possible to observe the discontinuous character of the softening variable that only evolves when the softening threshold Γ_{i_t} is attained, that is $\dot{\gamma}_i = 0$ and $\mathbf{N}_i : \bar{\dot{\mathbf{C}}} > 0$.

Finally, it would be interesting to see the effect of κ_i without the inclusion of the discontinuous damage for matrix and fibers. By comparing Figs. 4 and 2 it can see that the permanent set is equal in both cases and the softening very similar, however, the maximum stress of the change is higher in the model that does not consider the discontinuous damage, Fig. 4.

4.2. Anisotropic parameter analysis

In order to show the anisotropy characteristics of the proposed model, the formulation is used to simulate the behavior of a fiberd material with two perpendicular fiber directions using the QExp model (17). Uniaxial tests of an incompressible fiberd material are computed in *X*- and *Y*-directions. The material properties in each direction are different. Three cases are computed; Case 1 corresponds to equal elastic and different damage properties, Case 2 corresponds to different elastic and equal damage properties and Case 3 corresponds to different elastic and damage properties, see Table 2.

Fig. 5 shows the results for each case. For Case 1, when the elastic properties are equal and the softening ones different, it is possible to observe the anisotropic behavior in the softening phenomena. In the *X*-direction the softening and damage are lower due to fact that the inelastic material properties are lower. In Cases 2 and 3, where the elastic properties are different, the behavior of the tissue depends heavily on the direction of the test, showing a stiffer behavior in the *X*-direction.

Table 2
Material, damage and softening parameters for uniaxial simple tension. μ and k_1, k_3 are in MPa, γ_i is in $MPa^{1/2}$ and other parameters are dimensionless.

Case 1	μ	k_1	k_2	I_{4_0}	k_3	k_3	I_{6_0}	
	0.28	1.1226	1.5973	1.1	1.1226	1.5973	1.1	
	α_m	γ_m	α_{f_1}	γ_{f_1}	κ_{f_1}	α_{f_2}	γ_{f_2}	κ_{f_2}
	7.0	0.4	0.7	2.06	0.001	0.9	2.23	0.003
Case 2	μ	k_1	k_2	I_{4_0}	k_3	k_3	I_{6_0}	
	0.28	1.1226	1.5973	1.1	0.653	0.79568	1.1	
	α_m	γ_m	α_{f_1}	γ_{f_1}	κ_{f_1}	α_{f_2}	γ_{f_2}	κ_{f_2}
	7.0	0.4	0.7	2.06	0.001	0.7	2.06	0.001
Case 3	μ	k_1	k_2	I_{4_0}	k_3	k_3	I_{6_0}	
	0.28	1.1226	1.5973	1.1	0.653	0.79568	1.1	
	α_m	γ_m	α_{f_1}	γ_{f_1}	κ_{f_1}	α_{f_2}	γ_{f_2}	κ_{f_2}
	7.0	0.4	0.7	2.06	0.001	0.9	2.23	0.003

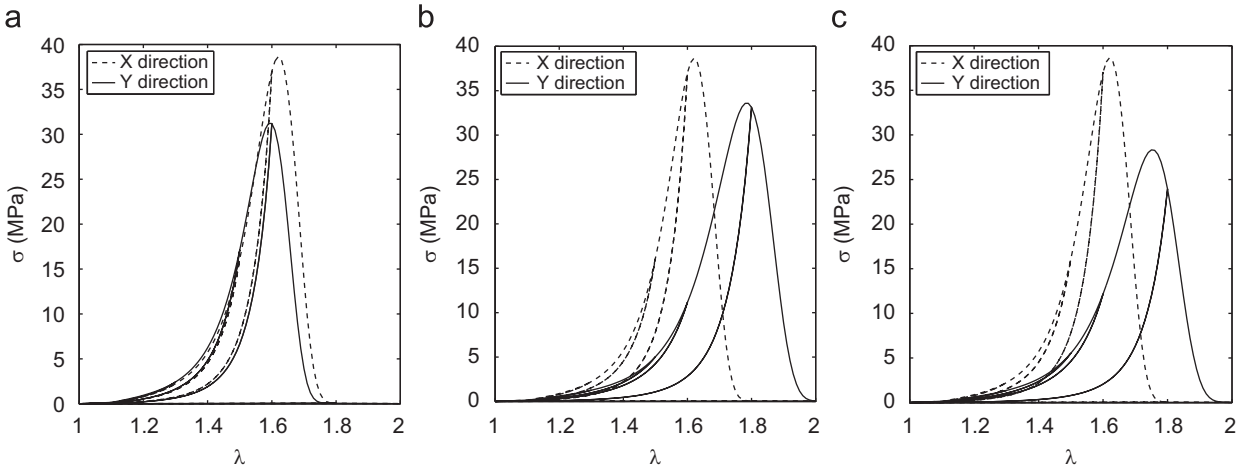

Fig. 5. Uniaxial stress response under cyclic uniaxial tension in *X*- and *Y*-directions. (a) Case 1, (b) Case 2 and (c) Case 3.

4.3. Application to soft biological tissues

To further assess the applicability of the proposed formulation, the prediction of the proposed model was compared with two sets of experimental data collected in our laboratory (Alastrué et al., 2008; Peña and Doblare, 2009).

The fitting of the experimental data was developed by using a Levenberg–Marquardt type minimization algorithm (Marquardt, 1963), frequently used in many other problems of experimental data fitting (Fung et al., 1979; Demiray et al., 1988; Hayashi, 1993). Convergence to the global minimum is difficult to achieve and the final results depend strongly on the initial guess. This problem has been noted previously and reported by Fung (1993) among many others. For this reason, the fits were performed several times starting with randomized parameters.

The tissue was assumed to be incompressible. The fitting procedure was performed minimizing the objective function represented in Eq. (37). In this function, σ_i is the Cauchy stress data obtained from the tests and $\sigma_i^{\tilde{\Psi}}$ is the Cauchy stresses for the *j*th point computed following Eq. (23), and n is the number of data points:

$$\chi^2 = \sum_{j=1}^{n} [\sigma_i - \sigma_i^{\tilde{\Psi}}]_j^2 \tag{37}$$

4.3.1. Inelastic effects in human vaginal tissue

These experiments were developed in our laboratory in order to study the properties of prolapsed human vaginal tissue. Longitudinal strips, approximately 6 mm wide and 15 mm long, were cut from each patient (Peña and Doblare, 2009). The whole vaginal wall, including mucosa, muscular layer and adventitia (Junqueira and Carneiro, 2007), was tested. Two circular black spots were painted on the surface of the strip to measure the deformation. Different loading and unloading cycles were applied (2, 4, 6 and 8 N) at 14%/min of strain rate in a high precision drive system, adapted for biological specimens (Instron Microtester 5548). The axial stretch ratio of the specimen was measured by a non-contacting laser video-extensometer Instron 2663-281. All tests were performed in a 100% humid atmosphere to prevent the specimens from drying out (Peña et al., 2011a). The elastic model was then fitted assuming that the tissue was incompressible and the SEF defined in (16) was considered.

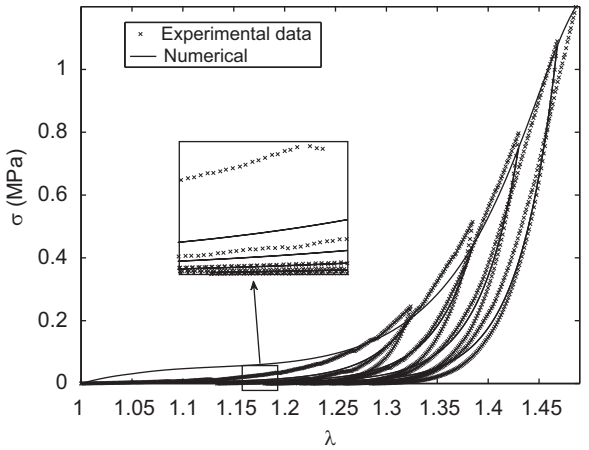

Fig. 6. Experimental and numerical simulation of loading and unloading curves at different load limits in vaginal tissue.

Table 3
Material, damage and softening parameters for vaginal sample. μ and c_1 are in MPa, γ_i is in $MPa^{1/2}$ and other parameters are dimensionless.

μ	c_1	c_2	I_{4_0}	
0.30	0.0103	8.8403	1.05	
α_m	γ_m	α_f	γ_f	κ
10.0	0	0.90	6.75	0.0333

The comparison between the experiments and the simulation for vaginal tissue are shown in Fig. 6. The corresponding material parameters are given in Table 3. The loading and unloading curves and the permanent stretch for each cycle are fitted. However, the computed primary loading curve has a higher deviation from the experimental data in the stretch region below 1.2, therefore the agreement in this region is moderate. This fact is due to that there seem to be a high derivation of the stress in the low stretch region in the primary curve related to the elastic model $\Psi^{\text{fib(i)}}$ rather than to the softening constitutive model. For this particular example, the residual stretch is low $\lambda_{perm} \approx 1.1$. However the softening parameter is high $\kappa = 0.0333$ due to the fact that $\bar{I}_{4_0} = 1.05$ is low. In the experimental measurements the unloading and subsequent reloading curves do not coincide as in the idealized Mullins effect described above due to the possible presence of viscoelastic effects. Since the resected tissue was in the longitudinal axis of the vagina, the matrix behavior was not totally characterized. Consequently, the associated damage parameters $\alpha_m = 10.0$ and $\gamma_m = 0.90$ cannot be physically obtained from these experiments and are chosen to minimize the error without a definite physiological meaning. Uniaxial tension experiments in only one direction are in general not sufficient to determine all material parameters associated with the anisotropic material model. In general, a test in the longitudinal direction determines mainly the behavior of the fibers. A uniaxial test in the transversal direction would be necessary to determine the matrix parameters. So, in the example case, both matrix and fiber parameters are fitted using the longitudinal test.

4.3.2. Inelastic effects in ovine vena cava tissue

In this example, we compare the model here presented with experimental stress–stretch data from uniaxial cyclic loading tests on vein tissue. These experiments were developed in our laboratory in order to study the properties of ovine vena cava tissue (Alastrué et al., 2008). Longitudinal strips, approximately 5 mm wide and 15 mm long, were resected in the circumferential and longitudinal directions where collagen and elastic fibers are predominately oriented respectively. Different loading and unloading cycles were applied (corresponding to values of the stress of 60, 120 and 240 KPa) at 15 mm/min of displacement rate. The maximum load for each cycle was progressively increased and then followed by an unloading cycle with a force value close to zero. Two families of fibers oriented in circumferential (collagen) and longitudinal (elastin) directions were considered and the mechanical behavior was reproduced using the SEF defined in (17).

The model was fitted to the experimental data using the representative set of uniaxial data in both axial and circumferential directions with the optimization procedure previously described. The optimized parameters obtained are included in Table 4 and experimental and numerical results for loading and unloading are shown in Fig. 7. The loading and unloading responses predicted by the model in circumferential and longitudinal directions are in good agreement with the experimental data. It can be observed, however, that there is not a very good agreement in the first and second cycles in the longitudinal direction where the response of the model is softer than the experimental one. The results of the

Table 4
Material, damage and softening parameters for cava tissue. μ and k_1, k_3 are in MPa, γ_i is in $MPa^{1/2}$ and other parameter are dimensionless.

Case 1	μ	k_1	k_2	I_{4_0}	k_3	k_3	I_{6_0}	
	0.03	0.1947	9.428	1.12	0.029	0.8994	1.2	
	α_m	γ_m	α_{f_1}	γ_{f_1}	κ_{f_1}	α_{f_2}	γ_{f_2}	κ_{f_2}
	40.18	0.0346	5.7	0.1621	0.0572	4.6248	0.1829	0.0591

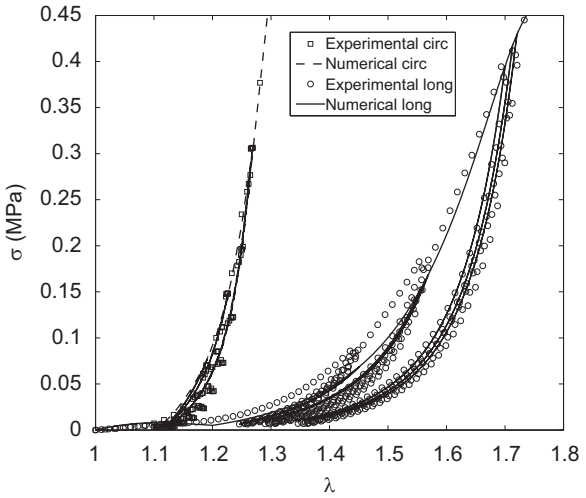

Fig. 7. Experimental and numerical simulation of loading and unloading curves at different load limits in cava tissue.

simulation clearly show that the fit carried out for the primary loading curve to obtain material constants in (17) cannot reproduce the initial region of the curve. The worse fit in the first and second cycles compared to the third could be explained by this phenomenon.

5. Conclusions

In the present paper, Mullins type behavior, damage and permanent set as a result of residual strains after unloading are captured using a novel constitutive model. We consider two weight factors w_i (softening) and s_k (discontinuous damage) as internal variables characterizing the structural state of the material with different evolution rule in matrix and fibers directions showing an anisotropic inelastic response. The proposed constitutive model successfully captures the main features of the inelastic response (softening, damage and permanent set) of soft fibered tissues. A good agreement of this model with recent experimental data on human vaginal tissue and cava sheep tissue has been achieved.

The present model has several advantages over previous inelastic models of soft biological tissues. As regards the classical continuum damage mechanics (CMD) formulations (Rodríguez et al., 2006; Calvo et al., 2007; Peña et al., 2009), our proposed model can reproduce the marked softening behavior of the soft tissues and the permanent set where the CMD fails (Chagnon et al., 2004; Guo and Sluys, 2006; Gracia et al., 2009). Pseudo-elastic models (Franceschini et al., 2006; Peña and Doblare, 2009) do not account for the permanent set and softening as a result of bond rupture and complete damage while the model presented is able to do so. However, the model by Franceschini et al. (2006) does account for the permanent applying the model by Dorfmann and Ogden (2004). Finally, Ehret and Itskov (2009) presented a model that reproduces the softening behavior including all the dissipative effects (including permanent set). However, the main drawback of this model is its use of non-standard invariants that leads to a very complicated approach and the model is not able to reproduce the damage process.

The mechanisms of the softening are not yet known, so the hypotheses of the model are purely phenomenological. The changes in the microstructure associated to w_i are structural alterations along the fibers direction such as the "waving" of the collagen fibers and represents a very simple framework to consider it. The changes in w_i also affect the softening phenomena during unloading and this is the reason to associate these internal variables to softening. We have hypothesized that the s_k are associated with discontinuous softening in matrix and fibers and w_i are associated with discontinuous softening in fibers as well as a residual deformation after unloading.

The limitations of the study include: (1) the need for a suitable experimental plan to obtain the many parameters involved; (2) the softening behavior of biological tissues is also related to viscoelastic effects; (3) the present model is phenomenological being very difficult to associate the internal variables w_i (softening) and s_k (discontinuous damage) with microstructural changes or internal processes; (4) one numerical problem concerning the finite element implementation should be addressed. This is related with the necessity of regularizing the ill-posed numerical problem (Bazant and Jirasek, 2002) where the loss of ellipticity/hyperbolicity of the governing equations with softening can lead to pathological mesh-sensitivity (Peña et al., 2011b).

However, a good qualitative agreement was found between numerical and experimental results, indicating that the constitutive inelastic model can capture the typical stress–strain behavior observed in fibrous soft tissue (Mullins effect or softening, damage and permanent set) with a minimal of softening material parameters (only three constants for each fiber direction). The availability of an accurate constitutive law to model soft fibered tissue response is a crucial requirement for assessing a local level of strain and stress associated to potential injury mechanics. Some possible fields of application may be mentioned such as sports (skiing, basketball, soccer) and traffic accidents, being the most important causes of ligament injury. Vascular surgery simulations (balloon angioplasty, arterial clamping or stenting), corneal laser interventions or plastic surgery are other interesting areas of application to be considered in the near future.

Acknowledgments

The author gratefully acknowledges research support from the Spanish Ministry of Science and Technology through the research projects DPI2010-20746-C03-01 and IPT-010000-2010-22, the Instituto de Salud Carlos III (ISCIII) through the CIBER initiative and Platform for Biological Tissue Characterization of the Centro de Investigación Biomédica en Red en Bioingeniería, Biomateriales y Nanomedicina (CIBER-BBN). CIBER-BBN is an initiative funded by the VI National R&D&i Plan 2008-2011, Iniciativa Ingenio 2010, Consolider Program, CIBER Actions and financed by the Instituto de Salud Carlos III with assistance from the European Regional Development Fund.

Appendix A. Derivation of the stress tensor

In this appendix we provide the explicit expressions for the stress tensors of the proposed model depending on the defined invariants. We only present the particularized form of the expressions used here, with I_5, I_7, I_8 and I_9 omitted.

The stress response is obtained from the derivatives of the stored-energy function for quasi-incompressible materials (Weiss et al., 1996):

$$\begin{aligned}\mathbf{S} = Jp\mathbf{C}^{-1} &+ 2J^{-2/3}[1-D_m]\left[\frac{\partial \Psi_{\text{ich}}}{\partial \bar{I}_1}\left[\mathbf{1}-\frac{1}{3}\bar{I}_1\bar{\mathbf{C}}^{-1}\right]-\frac{\partial \Psi_{\text{ich}}}{\partial \bar{I}_2}\left[\bar{I}_1\mathbf{1}-\mathbf{C}-\frac{2}{3}\bar{\mathbf{C}}^{-1}\right]\right]\\ &+2J^{-2/3}[1-D_{f_4}]\frac{\partial \Psi_{\text{ich}}}{\partial \bar{I}_4}\left[\bar{I}_4\mathbf{m}_0\otimes\mathbf{m}_0-\frac{1}{3}\bar{I}_4\bar{\mathbf{C}}^{-1}\right]+2J^{-2/3}[1-D_{f_6}]\frac{\partial \Psi_{\text{ich}}}{\partial \bar{I}_6}\left[\bar{I}_6\mathbf{n}_0\otimes\mathbf{n}_0-\frac{1}{3}\bar{I}_6\bar{\mathbf{C}}^{-1}\right]\end{aligned} \tag{A.1}$$

with $p=\partial\Psi_{\text{vol}}(J)/\partial\mathbf{C}$ the hydrostatic pressure.

For the generalized strain-energy function (6) with softening, the derivatives of the stored-energy function are computed as

$$\frac{\partial \Psi_{\text{ich}}}{\partial \bar{I}_1} = \mu_1+\frac{\gamma}{a\eta}[a\eta(\bar{I}_1-3)^{a-1}\exp(\eta[\bar{I}_1-3])^a-f'(\bar{I}_1,a)] \tag{A.2}$$

$$\frac{\partial \Psi_{\text{ich}}}{\partial \bar{I}_2} = \mu_2 \tag{A.3}$$

$$\left.\frac{\partial \Psi_{\text{ich}}}{\partial \bar{I}_i}\right|_{i=4,6} = \frac{c_{i-3}}{bc_{i-2}}[c_{i-2}b[\bar{I}_i-w_i\bar{I}_{i_0}]^{b-1}\exp(c_{i-2}[\bar{I}_i-w_i\bar{I}_{i_0}]^b)-g'(\bar{I}_i,\bar{I}_{i0},b)] \tag{A.4}$$

- For the *Exp* model the derivatives of the SEF are represented by

$$\frac{\partial \Psi_{\text{ich}}}{\partial \bar{I}_1} = \mu_1,\quad \frac{\partial \Psi_{\text{ich}}}{\partial \bar{I}_2} = 0,\quad \frac{\partial \Psi_{\text{ich}}}{\partial \bar{I}_4} = c_1[\exp(c_2[\bar{I}_4-w_4\bar{I}_{4_0}])-1] \tag{A.5}$$

- For the *QExp* model the derivatives of the SEF are represented by

$$\frac{\partial \Psi_{\text{ich}}}{\partial \bar{I}_1} = \mu_1,\quad \frac{\partial \Psi_{\text{ich}}}{\partial \bar{I}_2} = 0$$

$$\frac{\partial \Psi_{\text{ich}}}{\partial \bar{I}_4} = c_1[[\bar{I}_4 - w_4\bar{I}_{4_0}]\exp(c_2[\bar{I}_4 - w_4\bar{I}_{4_0}]^2)], \quad \frac{\partial \Psi_{\text{ich}}}{\partial \bar{I}_6} = c_3[[\bar{I}_6 - w_6\bar{I}_{6_0}]\exp(c_4[\bar{I}_6 - w_6\bar{I}_{6_0}]^2)] \tag{A.6}$$

The Cauchy stress tensor $\boldsymbol{\sigma}$ is $1/J$ times the push-forward of $\mathbf{S}$ ($\boldsymbol{\sigma} = J^{-1}\boldsymbol{\chi}_*(\mathbf{S})$. From (A.1), we obtain

$$\begin{aligned}\boldsymbol{\sigma} = p\mathbf{1} &+ \frac{2}{J}[1-D_m]\left[\frac{\partial \Psi_{\text{ich}}}{\partial \bar{I}_1}\left[\bar{\mathbf{b}} - \frac{1}{3}\bar{I}_1\mathbf{1}\right] - \frac{\partial \Psi_{\text{ich}}}{\partial \bar{I}_2}\left[\bar{I}_1\bar{\mathbf{b}} - \bar{\mathbf{b}}^2 - \frac{2}{3}\mathbf{1}\right]\right] \\ &+ \frac{2}{J}[1-D_{f_4}]\frac{\partial \Psi_{\text{ich}}}{\partial \bar{I}_4}\left[\bar{I}_4\mathbf{m}\otimes\mathbf{m} - \frac{1}{3}\bar{I}_4\mathbf{1}\right] + \frac{2}{J}[1-D_{f_6}]\frac{\partial \Psi_{\text{ich}}}{\partial \bar{I}_6}[\bar{I}_6\mathbf{n}\otimes\mathbf{n} - \frac{1}{3}\bar{I}_6\mathbf{1}]\end{aligned} \tag{A.7}$$

Appendix B. Derivation of the tangent tensor

Based on the kinematic decomposition of the deformation gradient tensor, the tangent operator, also known as the elasticity tensor when dealing with elastic constitutive laws, is defined in the reference configuration as

$$\mathbf{C} = 2\frac{\partial \mathbf{S}(\mathbf{C},\mathbf{M},\mathbf{N},D_k,w_i)}{\partial \mathbf{C}} = \mathbf{C}_{\text{vol}} + \mathbf{C}_{\text{ich}} = 4\left[\frac{\partial^2 \Psi_{\text{vol}}(J)}{\partial \mathbf{C}\otimes\partial \mathbf{C}} + \frac{\partial^2 \Psi_{\text{ich}}(\bar{\mathbf{C}},\mathbf{M},\mathbf{N},D_k,w_i)}{\partial \mathbf{C}\otimes\partial \mathbf{C}}\right] = \mathbf{C}_{\text{vol}} + \sum_{k=m,f_1,f_2}\left[[1-D_k]\mathbf{C}^0_{\text{ich}k} - \mathbf{S}_{\text{ich}k}\right] \tag{B.1}$$

where

$$\mathbf{S}_{\text{ich}k} = \begin{cases} [\dot{D}_k + \dot{w}_i q_i']\mathbf{S}_{\text{ich}k}\otimes\mathbf{S}_{\text{ich}k} & \text{if } \phi = 0 \text{ and } \mathbf{N}_k : \dot{\bar{\mathbf{C}}} > 0 \\ 0 & \text{otherwise} \end{cases} \tag{B.2}$$

To compute $\mathbf{S}_{\text{ich}k}$, it is necessary obtain the expression of q_i' for each strain-energy function.

- For the *Exp* model Eq. (13), q_i' is represented by

$$q_4' = \bar{I}_{40}\frac{c_2\exp(c_2[\bar{I}_4 - w_4\bar{I}_{40}])}{\exp(c_2[\bar{I}_4 - w_4\bar{I}_{40}]) - 1} \tag{B.3}$$

- For the *QExp* model Eq. (14), q_i' is represented by

$$q_i' = \bar{I}_{i0}\frac{2c_{i-2}[\bar{I}_i - w_i\bar{I}_{i0}]^2 + 1}{\bar{I}_i - w_i\bar{I}_{i0}} \tag{B.4}$$

Remark B.1. Note that the present formulation results in a symmetric algorithmic tangent modulus Eq. (B.1) with a low computational cost (Simo, 1987).

References

Alastrué, V., Peña, E., Martínez, M.A., Doblaré, M., 2008. Experimental study and constitutive modelling of the passive mechanical properties of the ovine infrarenal vena cava tissue. J Biomech 41, 3038–3045.

Baer, E., Cassidy, J.J., Hiltner, A., 1991. Hierarchical structure of collagen composite systems: lessons from biology. Pure Appl. Chem. 63, 961–973.

Balzani, D., Schröder, J., Gross, D., 2006. Simulation of discontinuous damage incorporating residual stress in circumferentially overstretched atherosclerotic arteries. Acta Biomater. 2, 609–618.

Bazant, Z.P., Jirasek, M., 2002. Nonlocal integral formulations of plasticity and damage: survey of progress. J. Eng. Mech. 128, 1119–1149.

Bonet, J., Wood, R.D., 2008. Nonlinear Continuum Mechanics for Finite Element Analysis. Cambridge University Press, Cambridge.

Calvo, B., Peña, E., Martins, P., Mascarenhas, T., Doblare, M., Natal, R., Ferreira, A., 2009. On modelling damage process in vaginal tissue. J. Biomech. 42, 642–651.

Calvo, B., Peña, E., Martínez, M.A., Doblaré, M., 2007. An uncoupled directional damage model for fibered biological soft tissues. Formulation and computational aspects. Int. J. Numer. Meth. Eng. 69, 2036–2057.

Chagnon, G., Verrona, E., Gorneta, L., Marckmanna, G., Charrierb, P., 2004. On the relevance of continuum damage mechanics as applied to the Mullins effect in elastomers. J. Mech. Phys. Solids 52, 1627–1650.

Ciarletta, P., Ben-Amar, M., 2009. A finite dissipative theory of temporary interf ibrillar bridges in the extracellular matrix of ligaments and tendons. J. R. Soc. Interface 6, 909–992.

Demiray, H., 1972. A note on the elasticity of soft biological tissues. J. Biomech. 5, 309–311.

Demiray, H., Weizsacker, H.W., Pascale, K., Erbay, H., 1988. A stress–strain relation for a rat abdominal aorta. J. Biomech. 21, 369–374.

Diamant, J., Keller, A., Baer, E., Litt, M., Arridge, R.G.C., 1972. Collagen: ultrastructure and its relation to mechanical properties as a function of aging. Proc. R. Soc. B: Biol. Sci. 180, 293–315.

Dorfmann, A., Ogden, R.W., 2004. A constitutive model for the Mullins effect with permanent set in particle-reinforced rubber. Int. J. Solids Struct. 41, 1855–1878.

Ehret, A.E., Itskov, M., 2009. Modeling of anisotropic softening phenomena: application to soft biological tissues. Int. J. Plasticity 25, 901–919.

Federico, S., 2010. Volumetric-distortional decomposition of deformation and elasticity tensor. Math. Mech. Solids 15, 672–690.

Flory, P.J., 1961. Thermodynamic relations for high elastic materials. Trans. Faraday Soc. 57, 829–838.

Franceschini, G., Bigoni, D., Regitnig, P., Holzapfel, G.A., 2006. Brain tissue deforms similarly to filled elastomers and follows consolidation theory. J. Mech. Phys. Solids 54, 2592–2620.

Fung, Y.C., 1993. Biomechanics. Mechanical Properties of Living Tissues. Springer-Verlag.

Fung, Y.C., Fronek, K., Patitucci, P., 1979. Pseudoelasticity of arteries and the choice of its mathematical expression. Am. J. Physiol. 237, H620–H631.

Gracia, L.A., Peña, E., Royo, J.M., Pelegay, J.L., Calvo, B., 2009. A comparison between pseudo-elastic and damage models for modelling the Mullins effect in industrial rubber components. Mech. Res. Commun. 36, 769–776.
Guo, Z., Sluys, L.J., 2006. Computational modelling of the stress-softening phenomenon of rubber-like materials under cyclic loading. Eur. J. Mech. A: Solids 25, 877–896.
Hayashi, K., 1993. Experimental approaches on measuring the mechanical properties and constitutive laws of arterial walls. ASME J. Biomech. Eng. 115, 481–488.
Helfenstein, J., Jabareen, M., Mazza, E., Govindjee, S., 2010. On non-physical response in models for fiber-reinforced hyperelastic materials. Int. J. Solids Struct. 47, 2056–2061.
Hokanson, J., Yazdami, S., 1997. A constitutive model of the artery with damage. Mech. Res. Commun. 24, 151–159.
Holzapfel, G.A., 2000. Nonlinear Solid Mechanics. Wiley, New York.
Holzapfel, G.A., Gasser, T.C., Ogden, R.W., 2000. A new constitutive framework for arterial wall mechanics and a comparative study of material models. J. Elasticity 61, 1–48.
Holzapfel, G.A., Ogden, R.W., 2009. Constitutive modelling of passive myocardium: a structurally based framework for material characterization. Philos. Trans. R. Soc. A 367, 3445–3475.
Horgan, C.O., Saccomandi, G., 2005. A new constitutive theory for fiber-reinforced incompressible nonlinearly elastic solids. J. Mech. Phys. Solids 53, 1985–2025.
Humphrey, J.D., 2002. Continuum biomechanics of soft biological tissues. Proc. R. Soc. London A 175, 1–44.
Hurschler, C., Loitz-Ramage, B., Vanderby, R., 1997. A structurally based stress–stretch relationship for tendon and ligament. ASME J. Biomech. Eng. 119, 392–399.
Ju, J.W., 1989. On energy-based coupled elastoplastic damage theories: constitutive modeling and computational aspects. Int. J. Solids Struct. 25, 803–833.
Junqueira, L.C., Carneiro, J., 2007. Basic Histology, eleventh ed. McGraw-Hill.
Li, D., Robertson, A.M., 2009. A structural multi-mechanism damage model for cerebral arterial tissue. ASME J. Biomech. Eng. 131, 101013 1–8.
Marquardt, D.W., 1963. An algorithm for least-squares estimation of nonlinear parameters. SIAM J. Appl. Math. 11, 431–441.
Marsden, J.E., Hughes, T.J.R., 1994. Mathematical Foundations of Elasticity. Dover, New York.
Miehe, C., 1995. Discontinuous and continuous damage evolution in Ogden-type large-strain elastic materials. Eur. J. Mech. A: Solids 14, 697–720.
Mooney, M., 1940. A theory of large elastic deformation. J. Appl. Phys. 11, 582–592.
Muñoz, M.J., Bea, J.A., Rodríguez, J.F., Ochoa, I., Grasa, J., del Palomar, A.P., Zaragoza, P., Osta, R., Doblaré, M., 2008. An experimental study of the mouse skin behaviour: damage and inelastic aspects. J. Biomech. 41, 93–99.
Natali, A.N., Pavan, P.G., Carniel, E.L., Dorow, C., 2003. A transverselly isotropic elasto-damage constitutive model for the periodontal ligament. Comp. Meth. Biomech. Biomed. Eng. 6, 329–336.
Natali, A.N., Pavan, P.G., Carniel, E.L., Luisiano, M.E., Taglialavoro, G., 2005. Anisotropic elasto-damage constitutive model for the biomechanical analysis of tendons. Med. Eng. Phys. 27, 209–214.
Ogden, R.W., 1996. Non-linear Elastic Deformations. Dover, New York.
Peña, E. A rate dependent directional damage model for fibred materials. Application to soft biological tissues. Comp Mech, in press, doi:10.1007/s00466-011-0594-5.
Peña, E., Alastrue, V., Laborda, A., Martínez, M.A., Doblare, M., 2010. A constitutive formulation of vascular tissue mechanics including viscoelasticity and softening behaviour. J. Biomech. 43, 984–989.
Peña, E., Doblare, M., 2009. An anisotropic pseudo-elastic approach for modelling Mullins effect in fibrous biological materials. Mech. Res. Commun. 36, 784–790.
Peña, E., Martins, P., Mascarenhas, T., Natal-Jorge, R.M., Ferreira, A., Doblaré, M., Calvo, B., 2011a. Mechanical characterization of the softening behavior of human vaginal tissue. J. Mech. Behav. Biomed. 4, 275–283.
Peña, E., Peña, J.A., Doblaré, M., 2009. On the Mullins effect and hysteresis of fibered biological materials: a comparison between continuous and discontinuous damage models. Int. J. Solids Struct. 46, 1727–1735.
Peña, J.A., Martínez, M.A., Peña, E., 2011b. A formulation to model the nonlinear viscoelastic properties of the vascular tissue. Acta Mech. 217, 63–74.
Rodríguez, J.F., Alastrue, V., Doblaré, M., 2008a. Finite element implementation of a stochastic three dimensional finite-strain damage model for fibrous soft tissue. Comput. Methods Appl. Mech. Eng. 197, 946–958.
Rodríguez, J.F., Cacho, F., Bea, J.A., Doblaré, M., 2006. A stochastic-structurally based three dimensional finite-strain damage model for fibrous soft tissue. J. Mech. Phys. Solids 54, 564–886.
Rodríguez, J.F., Ruiz, C., Doblaré, M., Holzapfel, G.A., 2008b. Mechanical stresses in abdominal aortic aneurysms: influence of diameter, asymmetry and material anisotropy. ASME J. Biomech. Eng. 130, 021023.
Simo, J.C., 1987. On a fully three-dimensional finite-strain viscoelastic damage model: formulation and computational aspects. Comput. Methods Appl. Mech. Eng. 60, 153–173.
Simo, J.C., Ju, J.W., 1987. Strain- and stress-based continuum damage models I. Formulation. Int. J. Solids Struct. 23, 821–840.
Simo, J.C., Taylor, R.L., 1991. Quasi-incompresible finite elasticity in principal stretches. Continuum basis and numerical algorithms. Comput. Methods Appl. Mech. Eng. 85, 273–310.
Simo, J.C., Taylor, R.L., Pister, K.S., 1985. Variational and projection methods for the volume constraint in finite deformation elasto-plasticity. Comput. Methods Appl. Mech. Eng. 51, 177–208.
Spencer, A.J.M., 1971. Theory of invariants. In: Continuum Physics. Academic Press, New York, pp. 239–253.
Tang, H., Moran, M.J.B.B., 2009. A constitutive model of soft tissue: from nanoscale collagen to tissue continuum. Ann. Biomed. Eng. 37, 1117–1130.
Vita, R.D., Slaughter, W.S., 2007. A constitutive law for the failure behavior of medial collateral ligaments. Biomech. Model Mechanbiol. 6, 189–197.
Volokh, K.Y., 2007a. Hyperelasticity with softening for modeling materials failure. J. Mech. Phys. Solids 55, 2237–2264.
Volokh, K.Y., 2007b. Prediction of arterial failure based on a microstructural bi-layer fiber-matrix model with softening. J. Biomech. 41, 447–453.
Volokh, K.Y., Vorp, D.A., 2008. A model of growth and rupture of abdominal aortic aneurysm. J. Biomech. 41, 1015–1021.
Weiss, J.A., Maker, B.N., Govindjee, S., 1996. Finite element implementation of incompressible, transversely isotropic hyperelasticity. Comput. Methods Appl. Mech. Eng. 135, 107–128.
Wulandana, R., Robertson, A.M., 2005. An inelastic multi-mechanism constitutive equation for cerebral arterial tissue. Biomech. Model Mechanbiol. 4, 235–248.
Zhou, J., Fung, Y.C., 1997. The degree of nonlinearity and anisotropy of blood vessel elasticity. Proc. Natl. Acad. Sci. USA 94, 14255–14260.